# Er-Doped Superfluorescent Fiber Source With a ±0.5-ppm Long-Term Mean-Wavelength Stability

Hee Gap Park, Michel Digonnet, *Member, IEEE,* and Gordon Kino, *Life Fellow, IEEE*

***Abstract*—We report an Er-doped superfluorescent fiber source (SFS) with a record mean-wavelength stability of ±0.5 ppm over 17 h. This breakthrough was achieved in a double-pass SFS by implementing several improvements, namely 1) controlling all the parameters that affect its mean wavelength, including the pump diode temperature and current, 2) reducing polarization-induced drifts in mean wavelength with a Faraday rotator mirror and a long Er-doped fiber (EDF), and 3) getting rid of polarization controllers to eliminate polarization-dependent loss. The long-term mean-wavelength variations of this SFS were due almost entirely to variations in the EDF temperature. When the SFS temperature was allowed to vary, by calibrating its mean-wavelength dependence on temperature, it was possible to predict the mean wavelength to a ±2-ppm precision by simply measuring the EDF temperature. The same configuration was also implemented with a different Er-doped fiber to achieve an even lower dependence on EDF temperature. When controlling the temperature of this second SFS to about ±0.5 °C, it exhibited a stability of ±0.5 ppm over 17 h. These new developments constitute an important step toward a practical high-grade fiber-optic gyroscope.**

***Index Terms*—Erbium, erbium-doped fiber (EDF), fiber-optic gyroscope (FOG), light sources, optical fiber lasers, stability, superfluorescense, wavelength measurement.**

## I. Introduction

Er-DOPED superfluorescent fiber sources (SFSs) have been studied extensively for their application in the fiber-optic gyroscope (FOG). These sources exhibit a unique combination of high efficiency, high spatial coherence, broad spectral emission, and excellent long-term stability of the mean wavelength [1]–[4]. This last property is important, because the scale factor of an FOG scales like the mean wavelength of the source, and accurate knowledge of the scale factor and, thus, of the mean wavelength is critical for accurate measurement of the absolute rotation rate. The state-of-the-art mean-wavelength stability for an Er-doped SFS is on the order of 8 ppm [2]. This is adequate for low- to medium-accuracy FOGs, but it is insufficient for high-accuracy inertial navigation FOGs, which require a stability of ∼1 ppm or better over many hours. The achievement of this goal has not yet been reported. One reason is that the mean wavelength of an SFS depends on many parameters, namely the wavelength, power, and polarization of the pump, the temperature and birefringence of the fiber, and the optical feedback returning from the FOG loop [1], [3], [4], and stabilizing all of these parameters is a difficult engineering task. This challenging 1-ppm objective has stimulated detailed studies of these individual contributions, and effective methods for reducing them have been reported [1]–[8]. The dependence on pump wavelength has been greatly reduced by selecting the pump wavelength appropriately [3], [7] and by stabilizing the laser diode temperature and current. The pump power dependence has been reduced by proper selection of the fiber length and pump power [2], [3] and by stabilizing the laser diode temperature and current. The effects of optical feedback can be reduced, and even cancelled, by proper design of the SFS configuration and by optically isolating the SFS and the gyro coil [3], [9]. These contributions have thus been reduced to the few ppm level or less.

The two largest remaining sources of instabilities are variations in the EDF-temperature and polarization-related effects. Temperature variations of the EDF modify the emission and absorption cross sections of erbium [10], which induces a drift in the mean wavelength [11]. The thermal coefficient depends not only on the EDF characteristics, but also on the configuration and operating parameters, in particular the pump wavelength and pump power [7]. Values ranging from −3 to 10 ppm/°C have been measured [2], [7], [12]. Although this effect is relatively weak, and optical filters can reduce it further [5], [6], [11], even a 1-ppm/°C value leads to unacceptably large mean-wavelength excursions because SFSs are required to operate over a wide temperature range (tens of degrees Celsius). It has also been suggested that with proper selection of the source parameters, it may be possible to design a double-stage SFS with a near-zero ppm/°C mean-wavelength dependence [13], although how close to zero has not been demonstrated. Polarization-related effects arise from the polarized nature of the pump light, which induces polarization-dependent gain (PDG) in the EDF [1], [14], [15]. Because of PDG, the two eigenpolarizations of the SFS output have substantially different mean wavelengths (in excess of 50 ppm) [14], [16]. Temperature and stress variations of any portion of fiber between the pump and the SFS output modify the fiber birefringence, which causes wandering of the pump polarization in the EDF and drift of the mean wavelength transmitted by the polarizer into the gyro coil. We speculate that this effect was responsible for at least some of the residual drift present in Hall's 8-ppm source [2]. We demonstrated that polarization-related drift can be greatly reduced with either Lyot depolarizers [14] or a Faraday rotator mirror (FRM) [15]. This last design reduces this drift to ∼20 ppm, but further improvements are clearly needed.

Manuscript received November 19, 2002; revised September 22, 2003. This work was supported by Northrop-Grumman. H. G. Park was supported in part by the Center for Electro-Optics, Korea.

H. G. Park is with the Department of Physics, Chonbuk National University, Chonju 561-756, Korea, and is also with the Edward L. Ginzton Laboratory, Stanford University, Stanford, CA 94305 USA.

M. Digonnet and G. Kino are with the Edward L. Ginzton Laboratory, Stanford University, Stanford, CA 94305 USA.

Digital Object Identifier 10.1109/JLT.2003.822539

Both the polarization-related effects and EDF-temperature effects could be drastically reduced by stabilizing the EDF temperature. However, this solution raises the power consumption, power-up time, size, and cost. An appealing alternative method is to calibrate the dependence of the SFS mean wavelength on the EDF temperature, then to measure the EDF temperature and use this value to compute the value of the mean wavelength. This method does not prevent the mean wavelength from drifting, but it enables the calculation of its value at any time. For this scheme to be successful, the SFS must be well stabilized, so that its mean wavelength depends only on the EDF temperature. If this requirement is not met, variations in temperature (and temperature gradients) will also affect other components of the SFS, in particular the fiber birefringence. The mean wavelength is then uncorrelated to the EDF temperature, and it is impossible to calibrate one against the other. Implementation of this technique has been hindered in the past by residual instabilities in the SFS arising from polarization-related effects [11].

In this paper, we report several design improvements in the double-pass FRM SFS that have led to the realization of an ultrastable source with a long-term mean-wavelength stability of $\pm 0.5$ ppm. First, as done in the past [17], a long Er-doped fiber was used to reduce PDG. Second, polarization controllers (PCs) were eliminated because they exhibit a small amount of polarization-dependent loss (PDL), which increases the apparent mean-wavelength dependence on polarization. Third, with these improvements in place, the SFS was found to be so stable that its long-term mean-wavelength variations were due almost entirely to variations in the EDF temperature. By measuring the ambient temperature over time (which is close to the EDF temperature), then correcting the mean wavelength measured at time $t = 0$ for the known thermal drift, we were able to predict the mean wavelength within $\pm 2$ ppm for 98 h. By using a different EDF in the same configuration, the thermal coefficient of the source was further reduced, allowing the demonstration of a stability of $\pm 0.5$ ppm over 17 h without correcting for EDF-temperature drifts ($\pm 0.5$ °C or greater). These two stability records constitute an important step toward a practical high-grade fiber-optic gyroscope.

## II. SFS Configuration Design and Principle

The SFS configuration used in this work is the double-pass forward source illustrated in Fig. 1. The active medium consisted of 94 m of EDF with a core radius of $\sim 1.1$ $\mu$m, an NA of 0.26, and a small-signal absorption at 1.53 $\mu$m of 3.7 dB/m. The pump source was a 1472-nm laser diode with 30 mW of fiber-pigtailed power, which was launched into the EDF through a wavelength-division-multiplexed (WDM) fiber coupler. The pumped EDF produces amplified spontaneous emission (ASE) both in the forward (away from the pump) and backward (toward the pump) directions. The backward ASE is directed by the WDM coupler to a fiber-pigtailed FRM, which reflects the backward ASE and sends it a second time through the EDF. The output isolator prevents time-dependent reflections from introducing undesirable fluctuations in the SFS mean wavelength. The SFS emitted 5 mW around 1550 nm and its linewidth, defined as in [2] and [3], was 17 nm.

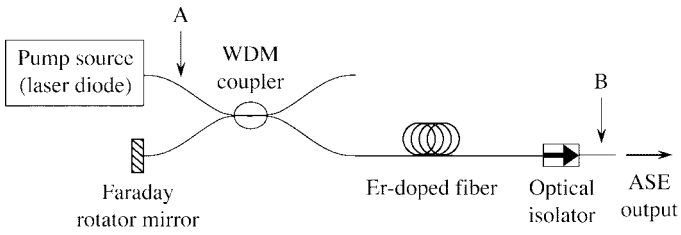


Fig. 1. Double-pass forward configuration of the Er-doped SFS, with FRM to reduce polarization-related mean-wavelength drifts.

A double-pass configuration was selected because it increases the SFS output power over a single-pass SFS and it generally reduces the EDF length requirement (note that the unusually long length (94 m) used in this experimental source is partly imposed by the fiber's low Er concentration). The use of a double-pass configuration also enables the elimination of polarization-related effects with an FRM (which is preferable over the long Lyot fiber depolarizers required to eliminate these effects in a single-pass SFS [14]). Because the pump is polarized, the Er-doped fiber exhibits PDG. If a standard reflector was used instead of an FRM, because of PDG, the two eigenpolarizations of the output ASE would have substantially different mean wavelengths [18]. Since there is a polarizer at the input to the FOG (to maintain reciprocity), thermal variations in the birefringence of either the EDF or the WDM fiber leads cause fluctuations in the mean wavelength of the signal transmitted by the polarizer into the gyro loop. The FRM solves this problem by guaranteeing that, at all points along the EDF, the polarization of the reflected backward ASE is orthogonal to that of the backward ASE, which cancels the effects of PDG [15].

One caveat of this technique is that the single-pass forward ASE component is not reflected by the FRM. Thus it does not experience polarization averaging, and its mean wavelength is still sensitive to polarization. This contribution is relatively small because the single-pass forward ASE has passed through the gain fiber only once, and thus carries considerably less power than the double-pass backward ASE. Nevertheless, the forward component is thought to be partly responsible for the $\sim$20-ppm residual mean-wavelength variations observed in our previous sources when perturbations were purposely applied to the EDF birefringence [15]. Modeling has shown that for very long EDF lengths, the polarization dependence of the FRM double-pass forward SFS becomes vanishingly small [17], which is the reason for selecting such a long EDF in this work. These theoretical predictions, as well as other theoretical predictions, were obtained using a computer model of SFS based on a standard three-level approximation of the Er ions and reported in detail elsewhere [3].

To reduce the mean-wavelength instabilities caused by variations in the pump wavelength $\lambda_p$, the temperature of the laser diode chip was controlled to $\pm 0.01$ °C. Since the measured temperature dependence of the laser diode wavelength was $\sim 1$ nm/°C, this corresponds to pump wavelength variations of $\Delta\lambda_p \approx \pm 0.01$ nm. (In the remainder of this paper, unless otherwise specified, all cited noise and fluctuation figures are peak-to-peak values.) In addition, the pump wavelength was temperature-tuned to 1472 nm, where modeling showed that

the first-order dependence of the SFS mean wavelength on pump wavelength cancels out [3]. Because the optimum pump wavelength probably differed slightly from this calculated value, a residual dependence of the SFS mean wavelength $\langle\lambda\rangle$ on temperature-induced variations in $\lambda_p$ was expected. This contribution was estimated via modeling, assuming that $\lambda_p$ departed from the optimum wavelength by 1 nm. The dependence of the mean wavelength on $\lambda_p$ was then calculated to be $\delta\langle\lambda\rangle/\delta\lambda_p \approx 0.015$. The SFS mean-wavelength variations due to temperature fluctuations of the laser diode were thus predicted to be only $\Delta\langle\lambda\rangle \approx \pm 0.00015$ nm ($\pm 0.1$ ppm), i.e., well under the 1-ppm target. This source of instability is therefore negligible.

Similarly, to stabilize the mean wavelength against pump power, the laser diode current was controlled to 10 $\mu$A, yielding a pump power stability of 1.3 $\mu$W. The calculated dependence of $\langle\lambda\rangle$ on pump power for this source is $-0.085$ nm/mW. Consequently, the pump power variations at the output of the laser diode have a negligible effect on the mean wavelength ($\sim$0.07 ppm). However, even though this input power is extremely stable, the pump power *launched* into the EDF can still fluctuate due to residual PDL in the WDM coupler, coupled to random variations in the pump polarization incident on the coupler caused by thermal variations in the fiber birefringence. For example, if the WDM coupler PDL is even as low as 0.01 dB, a 25-mW launched pump power $P_p$ will change by 0.05 mW as the pump polarization rotates by 90°. For the coefficient $|\partial\langle\lambda\rangle/\partial P_p|$ of this SFS ($-0.085$ nm/mW), the mean wavelength will vary by $\sim$3 ppm, which is excessive. However, a 90° rotation of the input pump polarization is unlikely to occur, and the SFS mean-wavelength variations due to this effect are likely going to be substantially smaller than 3 ppm. This figure of 3 ppm should therefore be regarded as a limit unlikely to be reached.

Nevertheless, two approaches were implemented to reduce this effect. First, the fiber pigtail between the laser diode and the EDF was shortened to reduce the total birefringence. Second, using manufacturers' data a WDM coupler with minimal PDL was selected. A third approach would be to reduce $|\partial\langle\lambda\rangle/\partial P_p|$ by proper selection of the fiber length and pump power [2], [3]. However, the length that minimizes $|\partial\langle\lambda\rangle/\partial P_p|$ may or may not be long enough to reduce the polarization dependence of the mean wavelength sufficiently. Modeling will be required in future work to elucidate this point and optionally to select an EDF length that strikes a suitable compromise between these two effects. In this work, as mentioned previously, a long EDF was selected in order to decrease polarization effects, but no attempt was made to study the effect of this longer length on $|\partial\langle\lambda\rangle/\partial P_p|$. As we shall see, this coefficient was still low enough to greatly improve the overall source stability.

In previous measurements on an FRM SFS, [15] polarization effects were tested by placing a PC at the output of the pump source (point A in Fig. 1) to vary the state of polarization (SOP) of the pump injected in the EDF. This type of PC was subsequently found to exhibit a PDL around 1.5 $\mu$m in the range of 0.01–0.1 dB, depending on the wavelength and the particular component. Consequently, adjusting the PC modified the launched pump power and, thus, the SFS mean wavelength. Assuming a PDL at 1480 nm of only 0.02 dB, the mean-wavelength variations introduced by the PC would be as large as 8 ppm, which is of the order of what was measured (10–22 ppm) [15]. Similarly, a second PC was placed at the SFS output (point B in Fig. 1) to measure the dependence of the mean wavelength on polarization [15]. Here again, residual PDL in the PC probably caused an erroneously high reading of the mean-wavelength instability. For this reason, in this work, PCs were eliminated (PCs are not needed to operate the SFS anyway). We therefore did not measure polarization effects *per se*. Instead, we allowed the temperature of the SFS fibers to fluctuate, as it would in a gyro, which caused (among other things) variations in the fiber birefringence and, thus, variations in the pump polarization.

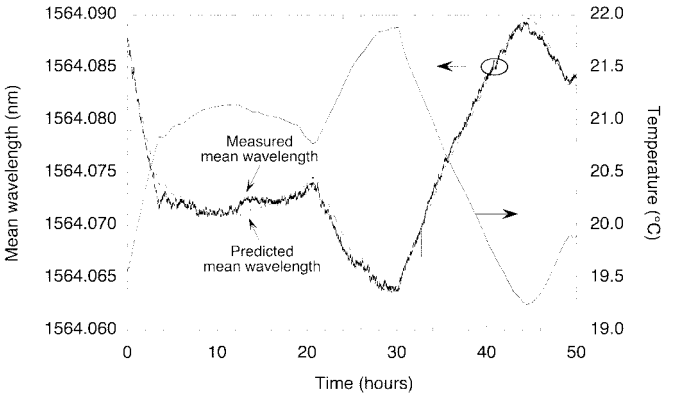


Fig. 2. Run 1: Mean wavelength of the SFS of Fig. 1 and room temperature recorded over a period of 50 h, and predicted mean-wavelength curve calculated from the fit of Fig. 3.

## III. Stability of the SFS Mean Wavelength With Correction of Thermal Drift

In this first set of measurements, the unpackaged SFS was placed on an optical table, and no attempts were made to control the temperature of either the room or the SFS fibers. An optical spectrum analyzer (OSA) recorded the SFS output spectrum every 19 sec for 50 h, and the mean wavelength of each spectrum was calculated with a computer. The OSA used in the measurements reported herein was an ANDO Model # AQ6327B. The wavelength resolution specified by the manufacturer is about $\pm 4.8$ ppm. Fig. 2 plots the evolution of the SFS mean wavelength and the room temperature measured during this run. The room temperature, and therefore the EDF temperature, varied over a range of 2.6 °C. As expected, because of these variations the mean wavelength also varied substantially ($\pm 8$ ppm). The two traces in Fig. 2 are obviously strongly correlated. Plotting the two quantities against each other (top trace in Fig. 3) shows that the mean wavelength varied almost linearly with temperature, as expected for a small perturbation. The small amount of hysteresis is likely due to a slight temperature lag between the measured room temperature and the actual EDF temperature. A linear fit to the data (top line in Fig. 3) yields the following dependence of the SFS mean wavelength $\langle\lambda\rangle$ (in nanometers) on room temperature $T$ (in degrees Celsius):

$$\langle\lambda\rangle = 1564.280\,55 - 0.0099149T. \quad (1)$$

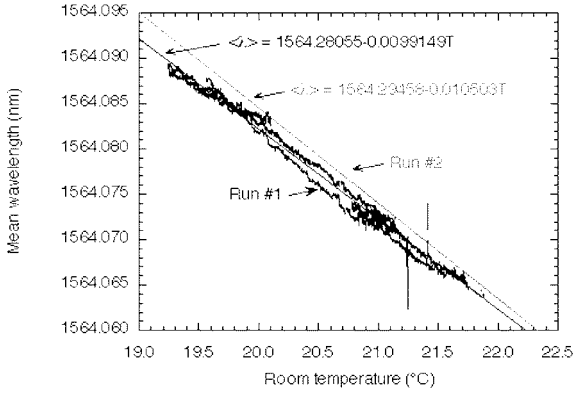


Fig. 3. Mean-wavelength plotted versus room temperature for run# 1 (lower trace) and run# 2 (top trace), and linear fit to each set of data.

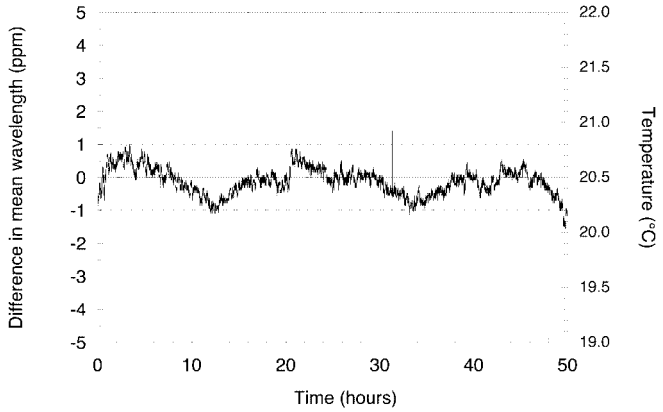


Fig. 4. Difference between measured mean wavelength and the mean wavelength predicted from the temperature curve of Fig. 1 and (1) (see text) for run# 1.

The SFS thermal coefficient ($-0.0099$ nm/°C, or $-6.3$ ppm/°C) is in the range of reported values [2], [7], [11], [12].

In a second step, we evaluated how well we could predict the mean wavelength of this SFS from the knowledge of its temperature alone. To do so, we applied (1) to the measured room temperature trace of Fig. 2. The result (dashed trace in Fig. 2) is in excellent agreement with the measured mean wavelength. This point is further illustrated in Fig. 4, which plots the difference between the measured and predicted mean-wavelength curves. This difference remains within $\pm 1$ ppm for the full 50 h of the test.

To confirm the validity of this method, the same measurement was repeated nine days later. We recorded the mean wavelength and room temperature for a 48-h period, plotted the mean wavelength versus temperature, and fitted it with a linear regression. This result is shown as the bottom trace and bottom line in Fig. 3. This second best linear fit is

$$\langle \lambda \rangle = 1564.29458 - 0.010503T. \tag{2}$$

We then used (2) to calculate the predicted mean wavelength from the measured temperature. The three curves are shown in Fig. 5. Again, the measured mean-wavelength and temperature curves are strongly correlated, and the measured and predicted

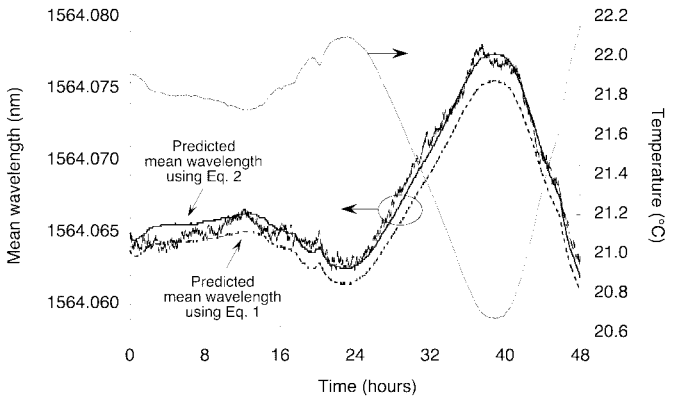


Fig. 5. Run# 2: Mean wavelength of the SFS of Fig. 1 and room temperature recorded over a period of 48 h, starting nine days after the end of run# 1. The smoother mean-wavelength curves were predicted using either (1) or (2), as labeled.

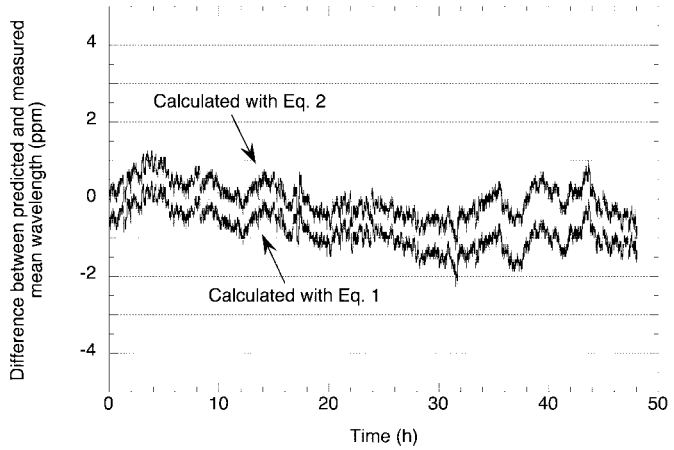


Fig. 6. Difference between the measured mean-wavelength trace of run# 2 and each of the two predicted mean-wavelength curves shown in Fig. 5.

mean-wavelength curves agree very well. The difference between these curves, shown as the top trace in Fig. 6, remained within $\pm 1$ ppm for 48 h.

These results show that by measuring the temperature of an SFS of known temperature dependence, one can compute its mean wavelength (and the gyro scale factor) accurately while the gyro is running. Since this temperature dependence obviously cannot be measured in real time, it needs to be measured beforehand. To evaluate how well this calibration technique works with this SFS, we considered the first run to be the "beforehand" calibration run, which provided the temperature dependence of (1), and we applied this dependence to the measured room-temperature evolution of the second run. The mean-wavelength evolution predicted in this manner is shown as the bottomr trace in Fig. 6. It has nearly the same form as the trace predicted using (2) (top curve), but it is shifted toward longer wavelengths. This shift has a mean value of 0.0013 nm ($\sim$1 ppm). Because of this offset, the error in the predicted trace is a little worse than before, but it still remains within $\pm 2$ ppm over the 48 h of the test.

The offset clearly originates from the small difference between the original thermal dependence (1) and the thermal dependence measured nine days later (2). Between the two runs,

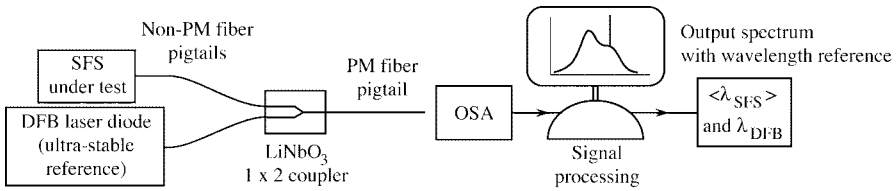


Fig. 7. Experimental setup used to measure the mean-wavelength stability of the second SFS. A highly stable DFB laser is used to calibrate the drift in the OSA.

the SFS was left untouched, so we speculate that this offset was mainly the result of a drift in the absolute wavelength reading of the OSA, whose temperature was not controlled. For this offset to be explained by the OSA drift, the latter would have to be around +1 ppm/°C. Unfortunately, measuring the OSA drift is extremely difficult because the wavelength of even an ultra-stable communication laser diode drifts by about the same amount (∼0.7 ppm) as the expected OSA drift. We are therefore currently unable to confirm this hypothesis.

We conclude that the proposed scheme works well, predicting the mean wavelength with a ±2 ppm accuracy over a 48-h period. This 2-ppm figure may be limited by the stability of the OSA, a point that needs to be confirmed.

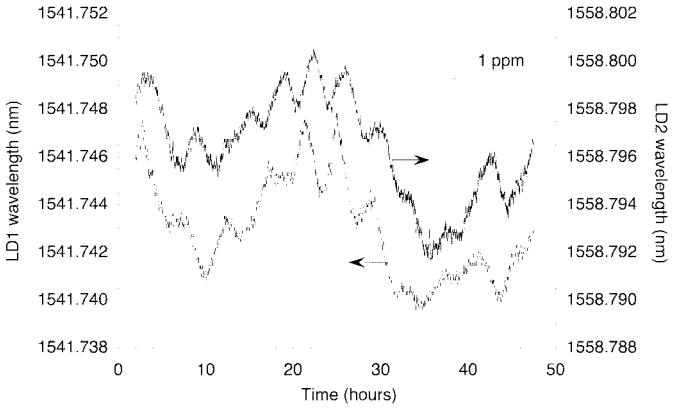


Fig. 8. Wavelength of two highly stable laser diodes recorded with the setup of Fig. 7 for a 48-h period.

## IV. Stability of the SFS Mean Wavelength With Temperature Control

The previous tests show that after correction for EDF-temperature variations, the SFS mean wavelength is constant within ±2 ppm. However, it does not tell us how stable the mean wavelength would be if the SFS temperature were constant. We would expect it to be even lower than ±2 ppm, since stabilizing the SFS temperature would eliminate not only the EDF thermal drift but other thermal effects as well, in particular fiber birefringence drifts and thus residual polarization-related effects. To address this issue, we present the results of a second series of stability tests in which the SFS temperature was kept relatively constant. The SFS was identical in all respects, except that the EDF was replaced with a fiber that produced a lower thermal coefficient. This second EDF had a length of 5.8 m, a core radius of 2.5 $\mu$m, an NA of 0.32, and a small-signal absorption at 1.53 $\mu$m of 25 dB/m. All source parameters were controlled to the same tolerance as described previously. The total small-signal absorption of this EDF at 1.53 $\mu$m was 145 dB, so polarization effects were also greatly suppressed. The EDF and the WDM coupler were placed in a Styrofoam enclosure to reduce their temperature fluctuations. The laboratory temperature was not tightly controlled, but the laboratory doors and windows were kept shut to minimize air currents. Room-temperature variations were estimated to be approximately ±0.5 °C.

As mentioned previously, a major difficulty in performing these tests is that the SFS wavelength stability was better than the stability of state-of-the-art commercial OSAs. To correct for the OSA long-term fluctuations, the OSA was calibrated using the scheme illustrated in Fig. 7. The SFS output and the signal from a highly stable wavelength reference were mixed in a fiber coupler and sent into the OSA. In the OSA trace, this reference is superposed on the SFS spectrum, and it provides an absolute calibration of the OSA wavelength scale. The reference source was a temperature-controlled WDM-communication-grade distributed feedback (DFB) laser diode (1541.74 nm) with a stability against case temperature variation better than 0.001 nm (0.7 ppm)/°C. Because the OSA response depends on polarization, we had to ensure that the polarization of the SFS signal launched into it did not vary over time. This was accomplished by using a lithium niobate Y-junction with a polarization-maintaining (PM) fiber pigtail as a coupler (see Fig. 7), which acted as a polarizer. Note that this scheme assumes that the drift in the OSA wavelength scale is uniform, i.e., that it is the same at all wavelengths across the SFS spectrum (∼1520 to ∼1580 nm), an assumption we examine further on.

The effectiveness of this calibration scheme and the validity of this uniform-drift assumption were checked by replacing the SFS by a second DFB laser diode (LD2) of similar wavelength and stability as the reference laser diode (LD1). Fig. 8 shows that the mean wavelengths of the two lasers, recorded simultaneously, both exhibit 1) short-term noise; 2) quasi-periodic oscillations with a period of 3–4 h and a peak-to-peak amplitude of ∼0.002 nm; and 3) overall quasiperiodic oscillations with a period of ∼24 h and a peak-to-peak amplitude of ∼0.005 nm. Each of these three components has a comparable magnitude for the two lasers. We believe that they are all a manifestation of OSA fluctuations on different time scales. The 3–4-h fluctuations can be explained if we assume that the OSA has a drift component that behaves as illustrated in Fig. 9. At a wavelength $\lambda_1$, the OSA reading fluctuates quasi-periodically with a period of 3–4 h and an amplitude of ∼0.002 nm. At a different wavelength ($\lambda_2$ or $\lambda_3$), the fluctuations have a comparable period and amplitude *but a different phase*. This behavior is consistent with the two wavelength recordings of Fig. 8, which are approximately out of phase. It is also consistent with our observation that the 3–4-h fluctuations are not present in OSA readings of the SFS mean

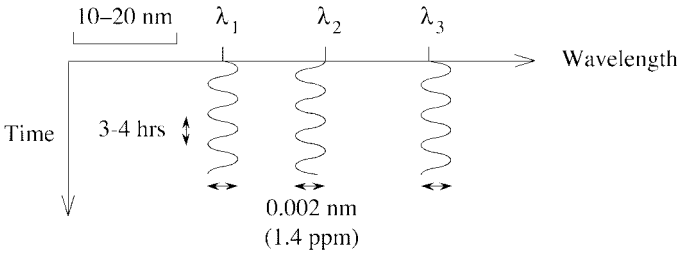


Fig. 9. Suggested mechanism explaining the temporal fluctuations of the OSA reading at three different wavelengths; fluctuations have comparable amplitude and period but different phases.

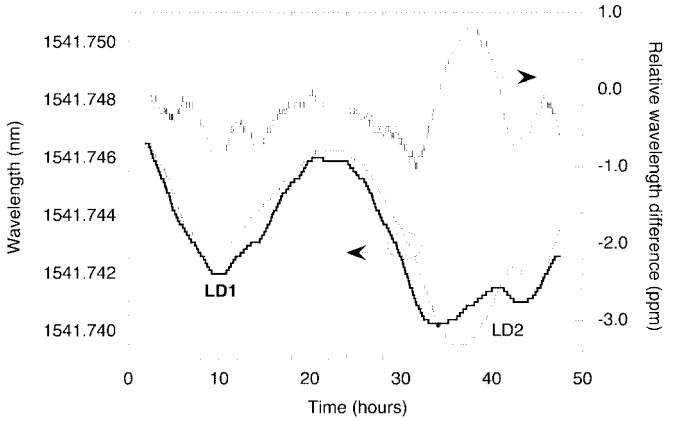


Fig. 10. Lower traces: wavelength traces of Fig. 8 after averaging out the 3–4-hour fluctuations due to the OSA. Upper trace: difference between the two lower traces, normalized to the average wavelength.

wavelength: the SFS spectrum is broad enough (a bandwidth greater than 10 nm) that these fluctuations are averaged out.

The third OSA drift component (period of ∼24 h) is believed to arise from periodic variations in the OSA temperature. To ascertain this statement, we averaged out each of the two curves in Fig. 8 with a ±3.5 h time window to get rid of the 3–4-h component. The smoothed curves are shown in Fig. 10 (the curve for LD2 was translated by −17 nm to bring it in the vicinity of the LD1 curve). It is now apparent that the 24-h oscillations of the two lasers are correlated. The difference between these two curves (top curve in Fig. 10) is constant within ±1 ppm. This calibration process therefore corrects for most of the OSA's original ±3 ppm long-term drift.

This scheme was used to measure simultaneously the variations in the mean wavelength of the SFS and in the wavelength of the reference diode (LD1) for 17 h. The laser diode trace was then smoothed as described previously. The two traces are presented in Fig. 11. As expected, their long-term variations are correlated, which proves that much of the variations in the SFS trace are due to long-term drift in the OSA. Fig. 12 displays the SFS trace after subtracting from it the LD1 trace to remove the OSA drift. It shows that the SFS exhibits a mean-wavelength stability of ±0.5 ppm over 17 h. The SFS short-term noise is under ±0.35 ppm (limited by the OSA). Since the SFS temperature variations during this run were estimated to be at least ± 0.5 °C, the thermal coefficient of this source was at most 1 ppm/°C, or about one order of magnitude smaller than the first SFS. The thermal coefficient of an SFS depends on many pa-

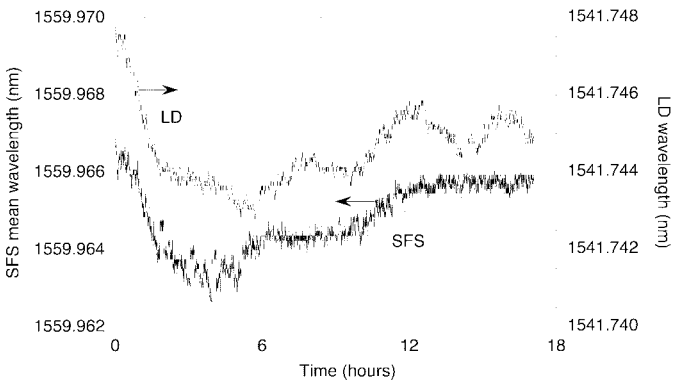


Fig. 11. SFS mean wavelength and laser diode wavelength recorded with the setup of Fig. 7 for a period of 17 h; each curve has been smoothed by integration (see text).

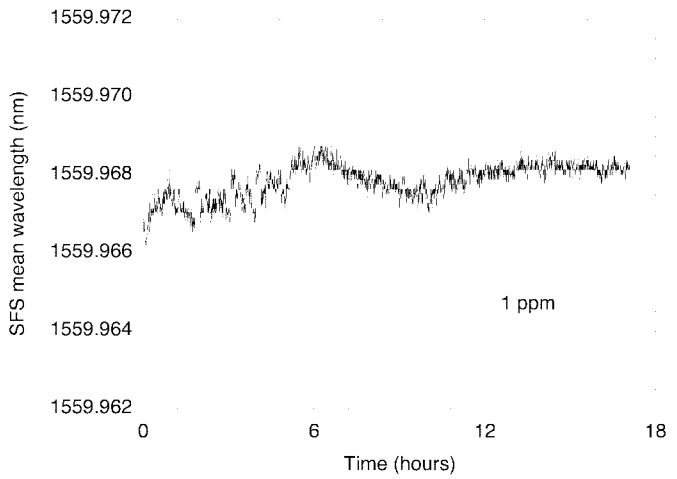


Fig. 12. SFS mean-wavelength trace of Fig. 11 corrected for the OSA long-term drift by subtracting from it the laser diode trace of Fig. 11.

rameters, including the configuration, the pump power, the EDF length, and the temperature dependence of the Er cross-section spectra. Simulations show that with proper choice of pump power and EDF length, the thermal coefficient cancels exactly [3]. The measured value of 1 ppm/°C or less is therefore not unexpected.

In these measurements, the stability of the sources was not tested against all possible SOPs of the pump input and ASE. This test would require the use of PCs, which introduce PDL and artificially increase the instability. Nevertheless, these measurements do show unambiguously that with SFS temperature excursions of ±0.5 °C, the birefringence in the SFS is stable enough to attain a stability of ±0.5 ppm.

## V. Conclusion

We have improved the mean-wavelength stability of the FRM double-pass forward SFS by careful source design, in particular to reduce residual polarization-related effects, and by stabilizing the pump wavelength and pump power. The SFS was stable enough that the only external parameter that affected its mean wavelength at a level greater than 1 ppm was temperature. This combined high stability and single-parameter dependence

made it possible, for the first time, to reproducibly measure the temperature dependence of the SFS mean wavelength. Over a long period of time (50 h), the mean wavelength was observed to vary almost linearly with temperature, with a thermal coefficient of about −0.01 nm/°C. Using this calibrated coefficient, we showed that the SFS mean wavelength could be predicted with an accuracy of ±2 ppm over a period of nearly 100 h by simply measuring the room temperature and calculating a correction term for the thermal drift. This is the first report of a SFS with a mean-wavelength long-term stability after calibration as low as ±2 ppm. Much of this residual drift was due to thermal drift in the wavelength reading of the OSA. To confirm this point, we ran a second series of tests in which 1) this drift was corrected by calibrating the OSA using a highly stable DFB laser diode as a wavelength reference, and 2) temperature variations of both the SFS and the OSA were lowered to around ±0.5 °C. The mean wavelength of the SFS was then found to exhibit a short-term noise under ±0.35 ppm (instrument limited) and a record long-term stability of ±0.5 ppm over 17 h.

These measurements show that by keeping the SFS temperature fluctuations within about ±0.5°C, the birefringence in the SFS is stable enough to attain a stability of ±0.5 ppm. When temperature excursions are larger, the mean wavelength can be calculated to within ±2 ppm (probably instrument limited) of its actual value by measuring the temperature of the SFS environment. This work demonstrates for the first time that it is possible to stabilize an Er-doped SFS well enough to meet the accuracy requirement of inertial navigation FOGs.

## REFERENCES


[1] D. G. Falquier, "Erbium doped superfluorescent fiber sources for the fiber optic gyroscope," Ph.D. dissertation, Applied Physics Dept., Stanford Univ., Stanford, CA, Dec. 2000.

[2] D. C. Hall, W. K. Burns, and R. P. Moeller, "High-stability $Er^{3+}$-doped superfluorescent fiber sources," *J. Lightwave Technol.*, vol. 13, pp. 1452–1460, July 1995.

[3] P. F. Wysocki, M. J. F. Digonnet, B. Y. Kim, and H. J. Shaw, "Characteristics of erbium-doped superfluorescent fiber sources for interferometric sensor applications," *J. Lightwave Technol.*, vol. 12, pp. 550–567, Mar. 1994.

[4] M. J. F. Digonnet, "Broadband fiber sources," in *Rare-Earth-Doped Fiber Lasers and Amplifiers*, 2nd ed, M. J. F. Digonnet, Ed. New York: Marcel Dekker, 2001, pp. 313–340.

[5] T. Gaiffe *et al.*, "Wavelength stabilization of an erbium-doped-fiber source with a fiber Bragg grating for high-accuracy FOG," in *Proc. SPIE*, vol. 2837, 1996, pp. 375–380.

[6] H. J. Patrick *et al.*, "Erbium-doped superfluorescent source with long period fibre grating wavelength stabilization," *Electron. Lett.*, vol. 33, no. 24, pp. 2061–2063, 1997.

[7] P. Wysocki, M. J. F. Digonnet, and B. Y. Kim, "Wavelength stability of a high-output, broadband, Er-doped superfluorescent fiber source pumped near 980 nm," *Opt. Lett.*, vol. 16, no. 12, pp. 961–963, June 1991.

[8] P. F. Wysocki, M. J. F. Digonnet, B. Y. Kim, and H. J. Shaw, "Broadband fiber sources for gyros," in *SPIE Proc. Fiber Optic Gyros: 15th Anniversary*, vol. 1585. Washington, DC, 1991, pp. 371–382.

[9] D. G. Falquier, "Erbium doped superfluorescent fiber sources for the fiber optic gyroscope," Ph.D. dissertation, Applied Physics Dept., Stanford Univ., Stanford, CA, Dec. 2000. pp. 80–94.

[10] J. Kemtchou and O. Ferres, "Absorption and emission cross-sections measurements for temperature dependent modeling of erbium-doped fibers amplifiers," in *Proc. Third Optical Fiber Measurement Conf.*, vol. 1, Liege, Belgium, 1995, pp. 76–80.

[11] D. G. Falquier, "Erbium doped superfluorescent fiber sources for the fiber optic gyroscope," Ph.D. dissertation, Applied Physics Dept., Stanford Univ., Stanford, CA, Dec. 2000.

[12] P. R. Morkel, "Erbium-doped fibre superfluorescent for the fibre gyroscope," in *Optical Fiber Sensors, Springer Proc.Phys.*, vol. 44, 1989, pp. 143–148.

[13] P. Z. Zatta and D. C. Hall, "Ultra-high-stability two-stage superfluorescent fibre sources for fibre optic gyroscopes," *Electron. Lett.*, vol. 38, no. 9, pp. 406–408, Apr. 2002.

[14] D. G. Falquier, M. J. F. Digonnet, and H. J. Shaw, "A depolarized Er-doped superfluorescent fiber source with improved long-term polarization stability," *IEEE Photon. Technol. Lett.*, vol. 13, pp. 25–27, Jan. 2001.

[15] ——, "A polarization-stable Er-doped superfluorescent fiber source including a Faraday rotator mirror," *IEEE Photon. Technol. Lett.*, vol. 12, pp. 1465–1467, Nov. 2000.

[16] D. G. Falquier, "Erbium doped superfluorescent fiber sources for the fiber optic gyroscope," Ph.D. dissertation, Applied Physics Dept., Stanford Univ., Stanford, CA, Dec. 2000. pp. 99–101.

[17] ——, "Erbium doped superfluorescent fiber sources for the fiber optic gyroscope," Ph.D. dissertation, Applied Physics Dept., Stanford Univ., Stanford, CA, Dec. 2000. Fig. 5.18 and pp. 118–119.

[18] J. L. Wagener, M. J. F. Digonnet, and H. J. Shaw, "A high-stability fiber amplifier source for the fiber optic gyroscope," *J. Lightwave Technol.*, vol. 15, pp. 1689–1694, Sept. 1997.


**Hee Gap Park**, photograph and biography not available at the time of publication.

**Michel Digonnet** (M'01) received the engineering degree from Ecole Supérieure de Physique et de Chimie de la Ville de Paris, France, the Diplome d'Etudes Approfondies degree in coherent optics from the University of Paris, Orsay, France, in 1978, and the M.S. and Ph.D. degrees in applied physics from Stanford University, Stanford, CA in 1980 and 1983, respectively. His doctoral research focused on wavelength-division-multiplexiing (WDM) fiber couplers and single-crystal fiber lasers and amplifiers.

From 1983 to 1986, he was employed by Litton Guidance and Control, Chatsworth, CA, as a Visiting Scholar at Stanford, conducting research in miniature solid-state sources and integrated optics for fiber sensors. From 1986 to 1990, he was involved in the development of dye and 2-$\mu$m solid-state lasers, fiber sensors, and delivery systems for laser angioplasty at MCM Laboratories, Mountain View, CA. Since then, he has been a Senior Research Associate in the Applied Physics Department, Stanford University. His current interests are rare-earth-doped fiber laser sources and amplifiers, nonlinear fiber devices, glass poling, photonic bandgap fibers, and fiber sensor arrays. He has published more than 150 articles, issued 50 patents, edited several books, and chaired multiple conferences on optical fibers and fiber sensors.

**Gordon Kino** (S'52–A'54–SM'63–F'66–LF'94) received the B.Sc. and M.Sc. degrees in mathematics from London University, London, U.K., and the Ph.D. degree in electrical engineering from Stanford University, Stanford, CA.

He was formerly the Director of the Ginzton Laboratory at Stanford University. He is the W. M. Keck Foundation Professor of Electrical Engineering, Emeritus, and Professor, by Courtesy, of Applied Physics, Emeritus. He has worked on microwave tubes, electron guns, plasmas, the Gunn effect, acoustic devices, acoustic imaging, nondestructive testing, fiber optics, and microscopy. His current interests are in various forms of near-field and scanning confocal microscopy, fiber optics, and optical storage. He has published more than 430 papers and has 47 patents. He and his students have developed new types of scanning optical microscopes and interferometric microscopes, and he and his students invented the Real-Time Scanning Confocal Optical Microscope, the Mirau Correlation Microscope, the Solid Immersion Lens for optical microscopy and storage, and a Micromachined Confocal Scanning Optical Microscope. Along with Timothy Corle, he is the author of *Confocal Optical Microscopy and Related Techniques* (New York: Academic, 1996), and he is the author of *Acoustic Waves: Devices, Imaging, and Analog Signal Processing* (Englewood Cliffs, NJ: Prentice-Hall, 1987).

Dr. Kino was a Guggenheim Fellow in 1967 and is currently a Fellow of the American Physical Society and the American Association for the Advancement of Science (AAAS), and a Member of the National Academy of Engineering. He received the IEEE Sonics and Ultrasonics Group Achievement Award in 1984 and the ASNT Achievement Award in Applied Research in 1986.